Global NEST Journal, Vol 23, No 3, pp 425-428

Synthesis of pyrene-based Fe(II)-complex and its photovoltaic properties

Erdoğan M.[1], Demirci S.[2], Adıgüzel V.[2], Horoz S.[3*] and Sait İzgi M.[4]
[1]Kafkas University, Faculty of Engineering and Architecture, Department of Food Engineering, Kars, 36100, Turkey
[2]Kafkas University, Faculty of Engineering and Architecture, Department of Chemical Engineering, Kars, 36100, Turkey
[3]Siirt University, Faculty of Engineering, Department of Electrical and Electronics Engineering, Siirt, 56100, Turkey
[4]Siirt University, Faculty of Engineering, Department of Chemical Engineering, Siirt, 56100, Turkey
Received: 06/06/2021, Accepted: 13/09/2021, Available online: 26/10/2021
*to whom all correspondence should be addressed: e-mail: sabithoroz@siirt.edu.tr
https://doi.org/10.30955/gnj.003754

Graphical abstract

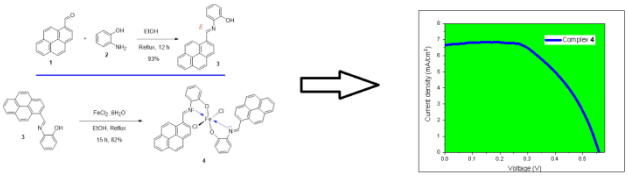

Abstract

(*E*)-2-((pyren-1-ylmethylene)amino)phenol (**3**) containing pyrene linked through an imine bond to a phenol unit was synthesized and its Fe-complex **4** was prepared. The complex **4** is characterized by infrared (IR), x-ray diffraction (XRD) and UV-Vis spectroscopy techniques. The synthesized complex was used as a sensitizer in a solar cell structure. From the current density (J)–voltage (V) curve obtained, the values of the short-circuit current density (J_{SC}), maximum current density (J_M), open-circuit voltage (V_{OC}) and maximum voltage (V_M) for the complex **4** were determined as 6.68 mA/cm^2, 4.73 mA/cm^2, 0.56 V and 0.41 V, respectively. Using these parameters, the fill factor (FF) and power conversion efficiency value (η) of complex **4** were calculated as 0.52 and 1.94, respectively. This value shows that complex **4** can be used as an effective sensitiser in solar cell applications.

Keywords: Pyrene; photovoltaic; imine; Fe (II) complex.

1. Introduction

Pyrene-based compounds are used in order to scan living cell by using their colorimetric and fluorescent characteristics as an optical sensor and as a chemoreceptor (Kushwaha *et al.*, 2018; Pinheiro *et al.*, 2014; Rasheed *et al.*, 2015; Shellaiah *et al.*, 2013; Tümay *et al.*, 2018). Pyrene is also used as a chemical sensor to detect chemicals such as neutral molecules, organic molecules, anionic and cationic analytes (Pinheiro *et al.*, 2014). Schiff bases include azomethine group (C=N) in their structures. They provide high coordination with the transition metals due to a pair of electrons orbiting the sp^2 hybrid of the N atom of this azomethine group (Altuntas *et al.*, 2021; Şahin *et al.*, 2020). Moreover, they are organic compounds that have an important place in the development of coordination chemistry because they form highly stable complexes (Erdoğan *et al.*, 2021; Güngördü Solğun *et al.*, 2018; Horoz *et al.*, 2018; Kapıcıoğlu *et al.*, 2020). Schiff base Fe-complexes, with due to high stability in different oxidation states, have a wide range of applications such as in industry, as catalysis in chemistry, as antifungal, antibacterial, antitumor and anticancer in biology, and pharmacology (Abdel-Rahman *et al.*, 2017; Haghverdi *et al.*, 2018, Joseph and Rani, 2017; Mahmoud *et al.*, 2018; Prasad *et al.*, 2019).

Dye-sensitized solar cells (DSSCs) are a cheaper alternative to the traditional semiconductor-based, crystalline solar cells due to their low manufacturing cost (Clifford *et al.*, 2011; Nazeeruddin *et al.*, 1993). Unlike traditional solar cells, the dye that is responsible for the light absorption process in DSSCs is isolated from the components involved in transporting carriers of charges (Clifford *et al.*, 2011). It was used many Ru(II)-polypyridins as sensitizers in DSSCs, achieving system efficiencies of more than 10% (Chen *et al.*, 2009; Kalyanasundaram and Grätzel, 1998; Nazeeruddin *et al.*, 1993). Substituting Ru(II) with environmentally friendly and earth-abundant Fe(II) in the polypyridyl dye will further reduce the cost of DSSCs. Ferrere and Gregg first showed the ability of Fe(II)-polypyridins to photosensitize TiO_2 in a system where dye is attached to TiO_2 through the carboxylic acid linker (Ferrere and Gregg, 1998). This mechanism displays band-selective sensitization from the originally excited short-lived metal to ligand charge transfer (MLCT) state, suggesting that sensitization is feasible even for complexes that lack long-lived excited photoactive state. The effect of solvent and various substituents on the absorption properties of TiO_2 was subsequently observed, showing that a carboxylic acid linker paires the dye to TiO_2 more efficiently than a phosphonic acid linker. In Fe complex-TiO_2 assemblies, Meyer *et al.* demonstrated mainly two

sensitization frameworks: (1) direct sensitization in which an electron is induced from the Fe(II) core directly into Ti(IV) sites on TiO_2 and (2) indirect sensitization concerning inter - facial electron transfer (IET) from the originally populated dye MLCT states into the TiO_2 conduction band (Yang *et al.*, 2000).

In this study, azomethine bridged pyrene phenol-based ligand is obtained from the reaction of pyrene aldehyde and 2-aminophenol. After the obtained ligand is characterized, Fe (II) complex is synthesized. The photovoltaic characteristics of this complex are examined.

2. Experimental

2.1. General remarks

All reactions were carried out under nitrogen and monitored by TLC. All solvents were dried and distilled before use. TLC was carried out on silica gel 60 HF254 aluminium plates (Fluka). Melting points are uncorrected. The one- and two-dimensional NMR spectra were recorded on a Bruker-400 spectrometer using tetramethylsilane as the internal reference. The NMR spectra were recorded at 25 °C and coupling constants (*J* values) are given in Hz. Chemical shifts are given in parts per million (ppm). IR spectra were recorded on Perkin Elmer FT-IR spectrometer. Absorption spectrometry was performed using a Perkin Elmer Lambda 35 spectrophotometer. Absorbance spectroscopy measurement was performed on 5 µM samples in CH_2Cl_2. The method we reported in our previous study was used for J-V measurements. The suspension of the complex **4** was used as the sensitizer (Erdoğan and Horoz, 2021).

*2.2. Preparation of ligand **3***

The ligand **3** were synthesized according to a previously reported method in the literature (Rasheed *et al.*, 2015).

Pyrene-1-carbaldehyde (**1**): ^{1}H NMR (400 MHz, $CDCl_3$) δ 10.77 (s, 1H), 9.41 (d, *J* = 9.4 Hz, 1H), 8.43 (d, *J* = 8.0 Hz, 1H), 8.32-8.27 (m, 3H), 8.26-8.19 (m, 2H), 8.14-8.03 (m, 2H). (see the Supplementary Material for details, Figure S1).

(E)-2-((Pyren-1-ylmethylene)amino)phenol (**3**): ^{1}H NMR (400 MHz, $CDCl_3$) δ 9.75 (s, 1H, imine H-C=N), 8.87 (d, *J* = 9.4 Hz, 1H), 8.79 (d, *J* = 8.1 Hz, 1H), 8.31 – 8.01 (m, 7H), 7.49 (dd, *J* = 7.9, *J* = 1.2 Hz, 1H), 7.42 (s, 1H, OH), 7.30-7.23 (m, 1H), 7.09 (dd, *J* = 8.1, *J* = 1.1 Hz, 1H), 7.04-6.97 (m, 1H). (see the Supplementary Material for details, Figure S2). IR (cm^{-1}): ν_{max} 3357, 3065, 3042, 3024, 2987, 1612, 1589, 1575, 1537, 1489, 1388, 1362, 1289, 1246, 1185, 1151, 848, 821, 744, 713.

*2.3. Preparation of Fe(II)-complex **4***

A solution of the ligand **3** (0.994 g, 3.090 mmol) in dry EtOH (30 mL) was added to a stirred solution of a mixture of $FeCl_2.6H_2O$ (0.300 g, 1.510 mmol) in distilled EtOH (10 mL) under N_2 atm. The resulting reaction mixture was heated for 15 h at reflux temperature. After being cooled to room temperature, the precipitate formed was filtered and washed several times with hot EtOH to give black solid complex **4** (yield 0.950 g, 82%). IR (cm^{-1}): ν_{max} 3006, 2989, 1575, 1474, 1392, 1275, 1261, 1233, 844, 764, 750, 710.

3. Results and discussion

3.1. Synthesis

Pyrene-1-carbaldehyde (**1**), which was commercially available, became the key structure that allowed us to prepare ligand **3**. As shown in Scheme 1, ligand **3** was synthesized according to a previously reported method via a one pot pyrene-1-carbaldehyde (**1**) and 2-aminophenol (**2**) condensation in ethanol with excellent yield (93%) (Rasheed *et al.*, 2015). Then, the complex **4** was obtained in one step from the ligand **3** (2 equiv.) by treatment with $FeCl_2.6H_2O$ (1 equiv.) under refluxing dry EtOH for 15 h in 82% yield (Scheme 1).

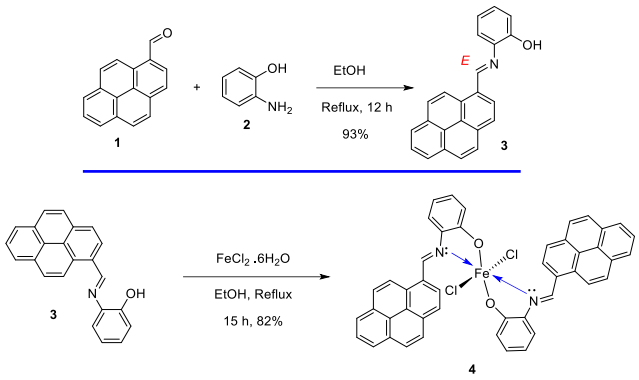

Scheme 1. Route of synthesis of Fe (II)-complex **4**.

3.2. FT-IR analysis

The IR spectrum of ligand **3** exhibited characteristic absorptions bands for -OH functional group, aromatic -C-H, imine -C=N-, and aromatic -C=C- bonds and no peaks attributable to unreacted amine or carbonyl groups (starting materials) were found.

The O-H stretch in phenolic unit is observed at 3357 cm^{-1}. The absorption bands at 2987, 3024 and 3042 cm^{-1} are attributed to aromatic C–H bending vibrations of compound **3**. The absorption band at 1612 cm^{-1} is assigned to stretching vibrations of the imine functional group, and those at 1589, 1575, 1537 and 1489 cm^{-1} are due to the aromatic C=C groups (see the Supplementary Material for details, Figure S3).

The IR spectrum of complex **4** exhibited characteristic absorptions bands for aromatic C-H, and aromatic C=C bonds. The absorption bands at 3006 and 2989 cm^{-1} are attributed to aromatic C–H bending vibration of the complex **4**. The absorption band at 1474 and 1575 cm^{-1} are assigned to the stretching vibration of the aromatic C=C groups. It was observed that the signal of the -OH functional group was disappeared (see the Supplementary Material for details, Figure S4).

3.3. UV-vis and XRD analysis

The result of the absorbance measurement for the complex **4** is shown in Figure 1. The UV-vis absorption spectra of the complex 4**,** in CH_2Cl_2 (5 µM) are dominated by absorption bands at the ligand **3**; 229, 233, 296 and 413, the complex **4**; 234, 289, 378, and 398 nm. As seen in Figure 1, the ligand **3** showed characteristic pyrene absorption peaks with their vibrational features. A peak observed at around 233 nm in the ligand **3** is attributed to $\pi \rightarrow \pi^*$ transition in the

aromatic rings, which remains almost unchanged in the metal complexes (234 nm).

Especially, a small hump observed in the region of 418-420 nm in the Fe(II) complex **4**. It may be the result of charge transfer from the imine nitrogen atom or oxygen atoms to the metal centre (Joseph and Rani, 2014).

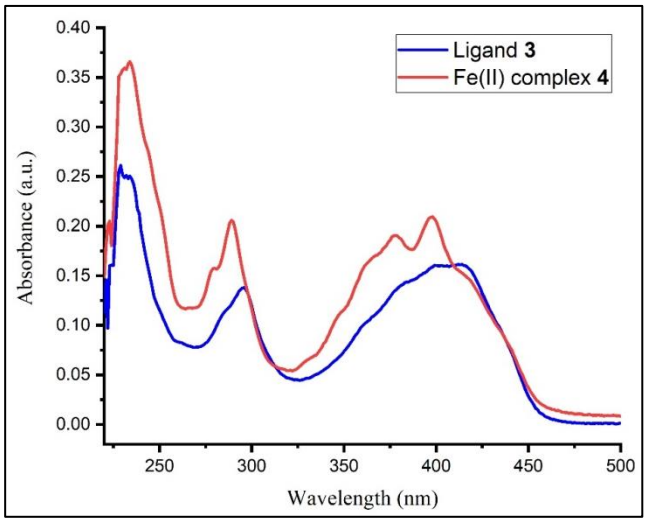

Figure 1. Plot of the wavelength versus absorbance intensity for complex **4**.

To obtain further information on the structure of the complex **4**, X-ray powder (XRD) diffraction was performed. The XRD patterns of the complex **4** is given Figure 2. As seen from the figure, the patterns are typical of amorphous structure of Fe-complex. Similiar result was reported by Zou *et al.* (2018).

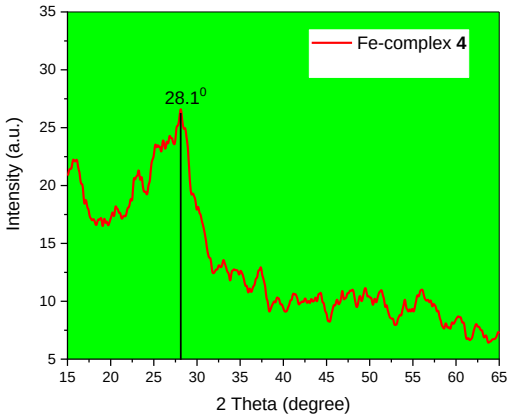

Figure 2. The XRD diffraction patterns of Fe(II) complex.

3.4. J-V measurement

Figure 3 shows the J-V curve of the synthesized complex **4**. Based on the J-V curve obtained, the values of the short-circuit current density (J_{SC}), maximum current density (J_M), open-circuit voltage (V_{OC}) and maximum voltage (V_M) for the complex **4** were determined as 6.68 mA/cm^2, 4.73 mA/cm^2, 0.56 V and 0.41 V, respectively. Using the equations (Eq.1 and Eq.2) given below (Şahin *et al.*, 2020), the fill factor (FF) and power conversion efficiency value (η) of complex **4** were calculated as 0.52 and 1.94, respectively.

$$FF = \frac{P_m}{J_{sc}V_{oc}} = \frac{J_M V_M}{J_{sc}V_{oc}} \quad (1)$$

$$\eta = \frac{P_m}{P_{in}} = \frac{J_{sc}V_{oc}FF}{P_{in}} \quad (2)$$

where P_m: maximum output power density, P_{in}: power density of incoming light.

It is well known that η% value of a DSSC device can be affected by the rate of electron transport in a solar cell structure. The obtained high J_{SC} value for complex **4** indicates that there is an effective injection of electrons into TiO_2 conduction band from excited state of complex dye. Thus, this leads to obtain improved conversion efficiency for complex **4** based-solar cell structure.

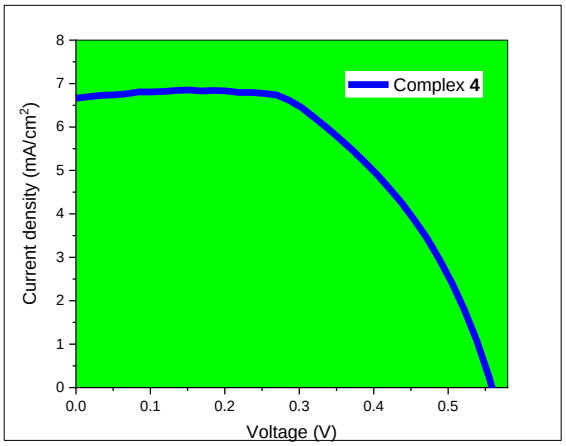

Figure 3. J-V curve of the complex **4**.

4. Conclusions

In summary, with azomethine bridge, a pyrene-phenol based ligand **3**, and its Fe-complex **4** were synthesized and characterized using spectroscopic methods. The complex was synthesized in good yield by simple condensation reaction. Additionally, the photovoltaic property of the complex **4** was investigated. The synthesized complex **4** was used as a sensitizer in a solar cell structure. The power conversion efficiency (%) of the complex **4** was calculated as 1.94 from the J-V curve obtained. This value shows that complex **4** can be used as an effective sensitizer in solar cell applications.

References

Abdel-Rahman L.H., et al. (2017). Synthesis, characterization, DFT calculations and biological studies of Mn (II), Fe (II), Co (II) and Cd (II) complexes based on a tetradentate ONNO donor Schiff base ligand. *Journal of Molecular Structure*, **1134**, 851–862.

Altuntas I., et al. (2021). Influence of the PALE growth temperature on quality of MOVPE grown AlN/Si (111). *Materials Science in Semiconductor Processing*, **127**, 105733.

Chen C.-Y., et al. (2009). Highly efficient light-harvesting ruthenium sensitizer for thin-film dye-sensitized solar cells. *ACS Nano*, **3**(10), 3103–3109.

Clifford J.N., et al. (2011). Sensitizer molecular structure-device efficiency relationship in dye sensitized solar cells. *Chemical Society Reviews*, **40**(3), 1635–1646.

Erdoğan M. and Horoz S. (2021). Synthesis and characterization of a triphenylamine-dibenzosuberenone-based conjued organic material and an investigation of its photovoltaic properties. *Journal of Chemical Research*, **45**(1–2), 207–212.

Erdoğan M. (2021). A novel dibenzosuberenone bridged DA-π-A type dye: Photophysical and photovoltaic investigations. *Journal of Molecular Structure*, **1232**, 130056.

Ferrere S. and Gregg B.A. (1998). Photosensitization of TiO_2 by [FeII(2,2′-bipyridine-4,4′-dicarboxylic acid)$_2$(CN)$_2$]: band selective electron injection from ultra-short-lived excited states. *Journal of the American Chemical Society*, **120**(4), 843–844.

Güngördü Solğun D., Horoz S., and Ağırtaş M.S. (2018). Synthesis of novel tetra (4-tritylphenoxy) substituted metallophthalocyanines and investigation of their aggregation, photovoltaic, solar cell properties. *Inorganic and Nano-Metal Chemistry*, **48**(10), 508–514.

Haghverdi M., et al. (2018). Preparation, characterization, DFT calculations and ethylene oligomerization studies of iron (II) complexes bearing 2-(1H-benzimidazol-2-yl)-phenol derivatives. *Journal of Coordination Chemistry*, **71**(8), 1180–1192.

Horoz S., Sahin O. and Ekinci A. (2018). Synthesis of Fe alloyed PbS thin films and investigation of their photovoltaic properties. *Journal of Materials Science: Materials in Electronics*, **29**(16), 13442–13448.

Joseph J. and Rani G.A.B. (2014). Metal-based molecular design tuning biochemical behavior: synthesis, characterization, and biochemical studies of mixed ligand complexes derived from 4-aminoantipyrine derivatives. *Spectroscopy Letters*, **47**(2), 86–100.

Kalyanasundaram K. and Grätzel M. (1998). Applications of functionalized transition metal complexes in photonic and optoelectronic devices. *Coordination Chemistry Reviews*, **177**(1), 347–414.

Kapıcıoğlu A. and Esen H. (2020). Experimental investigation on using Al_2O_3/ethylene glycol-water nano-fluid in different types of horizontal ground heat exchangers. *Applied Thermal Engineering*, **165**, 114559.

Kushwaha A., Patil S.K., and Das D. (2018). A pyrene-benzimidazole composed effective fluoride sensor: potential mimicking of a Boolean logic gate. *New Journal of Chemistry*, **42**(11), 9200–9208.

Mahmoud W.H., Mohamed G.G. and El-Sayed O.Y. (2018). Coordination compounds of some transition metal ions with new Schiff base ligand derived from dibenzoyl methane. Structural characterization, thermal behavior, molecular structure, antimicrobial, anticancer activity and molecular docking studies. *Applied Organometallic Chemistry*, **32**(2), e4051.

Nazeeruddin M.K., et al. (1993). Conversion of light to electricity by cis-X2bis (2, 2'-bipyridyl-4, 4'-dicarboxylate) ruthenium (II) charge-transfer sensitizers (X= Cl-, Br-, I-, CN-, and SCN-) on nanocrystalline titanium dioxide electrodes. *Journal of the American Chemical Society*, **115**(14), 6382–6390.

Pinheiro D., et al. (2014). From yellow to pink using a fluorimetric and colorimetric pyrene derivative and mercury (II) ions. *Dyes and Pigments*, **110**, 152–158.

Prasad K.S., et al. (2019). Photophysical properties and theoretical investigations of newly synthesized pyrene-naphthalene based Schiff base ligand and its copper (II) complexes. *Inorganica Chimica Acta*, **486**, 698–703.

Rasheed L., et al. (2015). Turn-on ratiometric fluorescent probe for selective discrimination of Cr^{3+} from Fe^{3+} in aqueous media for living cell imaging. *Chemistry–A European Journal*, **21**(46), 16349–16353.

Şahin Ö., Kilinç D., and Horoz S. (2020). A study on the ligand-bound Mn (II) complex. *Inorganic and Nano-Metal Chemistry*, **50**(4), 298–302.

Shellaiah M., et al. (2013). Novel pyrene-and anthracene-based Schiff base derivatives as Cu 2+ and Fe 3+ fluorescence turn-on sensors and for aggregation induced emissions. *Journal of Materials Chemistry A*, **1**(4), 1310–1318.

Tümay S.O., et al.(2018). A systematic series of fluorescence chemosensors with multiple binding sites for Hg (II) based on pyrenyl-functionalized cyclotriphosphazenes and their application in live cell imaging. *New Journal of Chemistry*, **42**(17), 14219–14228.

Yang M., Thompson D.W. and Meyer G.J. (2000). Dual pathways for TiO_2 sensitization by Na_2 [Fe (bpy)$(CN)_4$]. *Inorganic Chemistry*, **39**(17), 3738–3739.

Zhu X., et al. (2018). A supramolecular peptide polymer from hydrogen-bond and coordination-driven self-assembly. *Polymer Chemistry*, **9**(1), 69–76.